Journal of Sound and Vibration (1993) **168**(3), 479–505

INDIVIDUAL AND INTERACTIVE MECHANISMS FOR LOCALIZATION AND DISSIPATION IN A MONO-COUPLED NEARLY-PERIODIC STRUCTURE

M. P. CASTANIER AND C. PIERRE

Department of Mechanical Engineering and Applied Mechanics, The University of Michigan, Ann Arbor, Michigan 48109-2125, *U.S.A.*

(*Received* 12 *February* 1992, *and in final form* 6 *July* 1992)

The effect of structural damping on the dynamics of periodic and disordered nearly periodic systems is investigated. A chain of single-degree-of-freedom oscillators coupled by springs is used as a basic model of a mono-coupled periodic system. The dynamic response of the system to a harmonic excitation at the leftmost oscillator is considered. For a system with damping but no disorder (i.e., identical oscillators), an exact expression for the rate of exponential spatial amplitude decay is retrieved. It is found that the decay rate due to damping in a periodic system has a frequency dependence similar to that of the decay rate due to disorder in an undamped nearly periodic system. The magnitudes of the decay rates due to only damping or disorder are compared, and the concept of equivalent damping due to disorder is introduced. For systems with both disorder and damping, perturbation methods are used to find approximate expressions for the decay rate in the cases of strong and weak coupling between oscillators. It is shown that if the coupling is strong, the decay rates due to damping and disorder simply add up to produce the overall decay rate, and the effect of damping dominates. If the coupling is weak, however, the effects of damping and disorder on the overall decay are comparable in magnitude, and they interact in a more complicated manner.

1. INTRODUCTION

A periodic system consists of an assembly of identical elements, or subsystems, which are coupled in some identical fashion. An example of such a system would be a turbine blade assembly. Ideally, the individual blades are identical, and they are dynamically coupled through the hub and through aerodynamic effects.

The dynamics of periodic systems have been studied in detail for several decades, sparked by the work of Brillouin [1]. For harmonic excitations, periodic structures are known to exhibit some notable characteristics. In specific frequency bands, energy-carrying waves propagate unattenuated through the system, with only a change in phase from one subsystem to the next. These ranges of frequencies are called the *passbands*. The number of passbands corresponds to the number of degrees of freedom for each subsystem, and the number of left- and right-travelling wave pairs is that of coupling co-ordinates between subsystems.

For frequencies outside the passbands, the wave—or vibration—amplitudes decay exponentially along the assembly. From one subsystem to the next, the amplitude is attenuated by a factor of $e^{-\gamma}$, where γ is the (positive) exponential decay constant.

0022-460X/93/270479 + 27 $08.00/0

The ranges of frequencies outside of the passbands are called the *stopbands*. (Note that for multi-coupled structures, complex waves may exist, which feature both attenuation and a phase change.) This passband–stopband behavior was examined extensively by Mead [2].

Of course, actual physical periodic systems tend to have discrepancies between the subsystems, or bays, even though they are intended to be identical. Material tolerances, manufacturing defects or other flaws invariably cause differences between the subsystems. These irregularities are referred to as disorder, or mistuning. It turns out that even slight disorder can have a drastic effect on the dynamics of the nominally periodic system, provided that the coupling between the subsystems is sufficiently weak or that the structure's modal density is large enough.

In particular, the deviation from periodicity leads to partial reflections of the energy-carrying waves at each bay. The energy therefore tends to be confined in a region near the excitation source. This pehnomenon is known as *localization*, and it was first noted by Anderson [3] in the field of solid state physics. Anderson's work was applied to the vibration of nearly periodic engineering structures by Hodges [4], who showed that the degree of localization depends on the ratio of disorder strength to coupling strength. Since then, there have been several analytical [5–10] and very few experimental [11, 12] studies of this phenomenon in particular structural systems (for a review of work on localization in the field of applied mechanics, the reader is referred to [13]).

Localization leads to a spatial decay in the vibration amplitude, even at frequencies which are within the passbands of the tuned system. This decay, when averaged over many configurations of random disorder, is known to be exponential, and the associated exponential decay constant is called the *localization factor*. Both random matrix theory [14] and stochastic perturbation methods [15, 16] have been used to find analytical approximations for the localization factor of mistuned–undamped systems.

In this paper the effects of disorder *and structural damping* on the dynamics of mono-coupled nominally periodic engineering structures are investigated. Since all engineering structures have some damping, it is important to understand how the effects of mistuning and dissipation interact. To date, only two studies have attempted to consider this interaction. Cai and Lin [17] considered damping in formulating localization factors for a mono-coupled system, but only the formulation was presented and no results were obtained for the damped structure. More recently, Lust *et al.* [18] included damping in finite element models of disordered multi-span beams and multi-bay trusses. Their numerical results showed that a reasonable value of damping made the responses of ordered and disordered structures nearly identical. Here, we find this to be true only for strongly coupled systems.

This paper provides both an analytical and numerical examination of localization for a simple theoretical model of a disordered and damped nearly periodic structure. It is shown that if damping and disorder are both large compared to the internal coupling, then they will both contribute substantially to the spatial vibration amplitude decay, although their effects do not simply add up. However, if damping and disorder are both small compared to the internal coupling, and they are of the same order of magnitude, then damping effects will dominate. This means that weak localization effects are unimportant in engineering structures.

The paper is organized as follows. In section 2, the derivation of the localization factor for the mistuned–undamped system is reviewed, using the model of reference [16]. In section 3, the disorder is removed from this model and structural damping is added. Unlike the mistuned system, an *exact* expression for the exponential decay constant of the

tuned–damped system is retrieved. In section 4 the system contains both damping and mistuning. Analytical expressions for the cases of strong and weak coupling are derived, and these are compared to Monte Carlo results. Also, the dynamic behavior of the mistuned–damped system for individual realizations of disorder is explored. Finally, section 5 presents the conclusions drawn from this study.

2. UNDAMPED SYSTEMS

2.1. THE TUNED–UNDAMPED SYSTEM

As a simple model of a perfectly periodic—or tuned—structure, let us consider a chain of identical, coupled oscillators with fixed–fixed boundary conditions, as shown in Figure 1. The assembly is excited at the leftmost oscillator by a harmonic force input of amplitude F and frequency ω. This oscillator, experiencing an external excitation, will be referred to as the first oscillator. The next oscillator to the right is the second oscillator, and so on. Each oscillator can be viewed as a massless beam of stiffness k_0, with a mass m concentrated at the tip. The oscillators are equally spaced and connected by springs of uniform coupling stiffness, k_c. Each oscillator undergoes a harmonic tip displacement of amplitude u_i, where i denotes the ith oscillator in the chain. The equations of steady state motion are, therefore,

$$-\omega^2 m u_i + (k_0 + 2k_c)u_i - k_c u_{i-1} - k_c u_{i+1} = F\delta_i^1, \qquad i = 1, \ldots, N, \tag{1}$$

where $\delta_i^1 = 1$ for $i = 1$, and is zero otherwise.

The coefficients of the left side of equation (1) are made dimensionless by dividing each side by the nominal oscillator's stiffness. We therefore introduce the following: $\omega_0 = \sqrt{k_0/m}$, the natural frequency of an individual oscillator; $\bar{\omega} = \omega/\omega_0$, the dimensionless excitation frequency; $R = k_c/k_0$, the dimensionless coupling; and $\bar{F} = F/k_0$, the modified force amplitude. The equations of motion become

$$(1 + 2R - \bar{\omega}^2)u_i - Ru_{i-1} - Ru_{i+1} = \bar{F}\delta_i^1, \quad i = 1, \ldots, N. \tag{2}$$

The propagation of waves through the associated infinite periodic structure can be examined as follows. Defining a bay of the periodic structure by an oscillator and the coupling spring to its right, the dynamics of the ith bay can be described by the vibration amplitude state vector $[u_i, u_{i-1}]^T$. State vectors for two adjacent bays are related by a

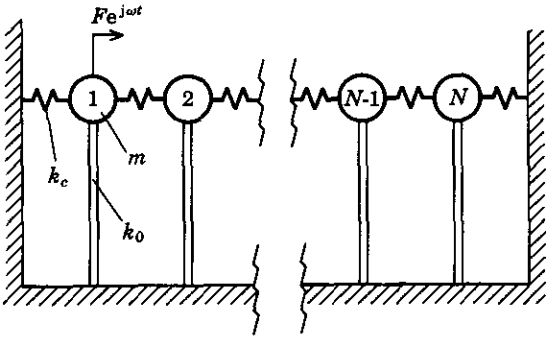

Figure 1. A schematic representation of the system of N mono-coupled one-degree-of-freedom oscillators, with a harmonic force excitation $F e^{j\omega t}$ at the first oscillator.

transfer matrix:

$$\begin{bmatrix} u_{i+1} \\ u_i \end{bmatrix} = [T_0] \begin{bmatrix} u_i \\ u_{i-1} \end{bmatrix}, \qquad [T_0] = \begin{bmatrix} 1 + 2R - \bar{\omega}^2 & -1 \\ R & \\ 1 & 0 \end{bmatrix}. \tag{3}$$

The displacement transfer matrix $[T_0]$ is uniform for all bays throughout the chain.

From the appendix, we know that the rate of exponential decay per bay (the real part of the propagation constant) of a harmonic wave propagating through the structure is

$$\gamma = \ln |\lambda_1|, \qquad |\lambda_1| \geqslant 1, \tag{4}$$

where λ_1 is an eigenvalue of $[T_0]$. Solving for the eigenvalues of the transfer matrix, we retrieve the expression

$$\gamma = \ln |(1/2R)[1 + 2R - \bar{\omega}^2 \pm \sqrt{(1 - \bar{\omega}^2)(1 + 4R - \bar{\omega}^2)}]|, \tag{5}$$

where, in order to retrieve the largest eigenvalue, the radical is either added or subtracted, depending on the frequency. Note that for $1 < \bar{\omega}^2 < 1 + 4R$, the radicand is negative and thus λ_1 is complex. Furthermore, when λ_1 is complex, $|\lambda_1| = 1$. Therefore $\gamma = 0$ and waves travel without spatial attenuation. This range of frequencies is called the *passband.* The passband edges for this system are therefore $\bar{\omega}^2 = 1$ and $\bar{\omega}^2 = 1 + 4R$. The free vibration natural frequencies of the finite structure belong to the passband. For $\bar{\omega}^2 < 1$ or $\bar{\omega}^2 > 1 + 4R$, λ_1 is real and $|\lambda_1| > 1$. For these frequencies $\gamma > 0$, and the system exhibits spatial wave amplitude decay. These regions of the frequency spectrum are called the *stopbands.*

2.2. THE MISTUNED–UNDAMPED SYSTEM

There is direct transmission of a wave through each bay of a tuned system. This transmission may be complete, or it may exhibit attenuation of the wave amplitude, but there is no scattering involved. In a mistuned system, however, there is both partial transmission and reflection at each site. For a mistuned chain of oscillators with a wave incident from the left, the multiple scatterings along the chain will tend to confine the energy near the left end of the mistuned segment. This phenomenon is appropriately referred to as *localization.*

Localization can also be viewed in terms of mode shapes. A tuned system is characterized by extended, periodic mode shapes. However, for a mistuned system with weak coupling, the effects of disorder can be quite remarkable, localizing the mode shape in a small region of the system. An example of this phenomenon is shown in Figure 2. For a local source of forced excitation, the response will tend to be confined near the source, since mode shapes localized in regions away from the energy source generally will have small amplitude at the source and therefore will not be greatly excited.

The forced response pattern varies for a chain of oscillators, depending on the distribution and magnitude of the disorder. On the average, the system exhibits an exponential spatial decay of the vibration amplitude along the chain. The averaged rate of decay per bay, γ_m, is called the *localization factor*, and is denoted here by the subscript m because it is associated with a mistuned system.

Disorder is introduced to the previous model by allowing each oscillator to have a different stiffness k_i. The value of the stiffness is considered to be uniformly distributed about the mean, k_0, with standard deviation σ, and half-width of the distribution, W (note that $W = \sqrt{3}\sigma$). In this way, σ can be used as a measure of the magnitude of the disorder present in the system. In order to account for these non-uniform values of stiffness, we

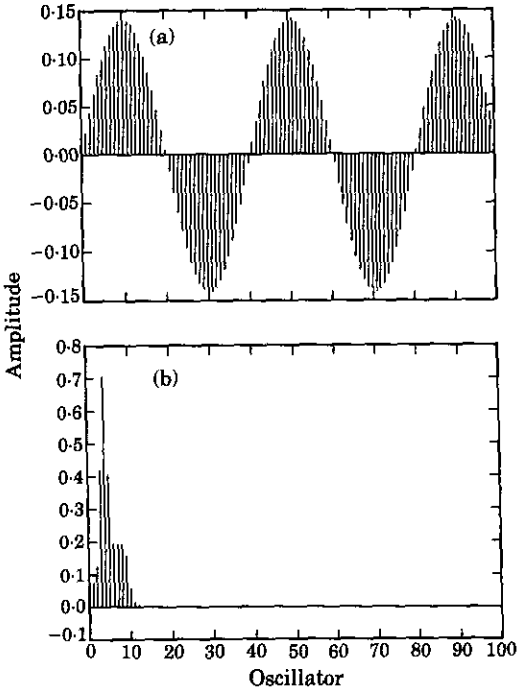

Figure 2. (a) The fifth mode shape of a tuned 100-oscillator system, with coupling $R = 0{\cdot}1$. (b) The fifth mode shape of a mistuned 100-oscillator system, with coupling $R = 0{\cdot}1$, and standard deviation of uniform random disorder $\sigma = 10\%$. The mode shape of the tuned system is extended, while the mode shape of the mistuned system is localized.

define the dimensionless variable $\Delta f_i = (k_i - k_0)/k_0$, the fractional deviation from mean stiffness. Therefore, for a disordered bay, equation (3) becomes

$$\begin{bmatrix} u_{i+1} \\ u_i \end{bmatrix} = [T_i]_m \begin{bmatrix} u_i \\ u_{i-1} \end{bmatrix}, \qquad [T_i]_m = \begin{bmatrix} \dfrac{1 + 2R - \bar{\omega}^2 + \Delta f_i}{R} & -1 \\ 1 & 0 \end{bmatrix}. \tag{6}$$

Here, $[T_i]_m$ is a random displacement transfer matrix for the ith bay.

The matrix of eigenvectors of $[T_0]$—which we will call $[P]$—can be used to transform the displacement transfer matrix into a wave transfer matrix via a similarity transformation. The global wave transfer matrix for an N-bay segment is

$$[\mathscr{W}_N]_m = \prod_{i=N}^{1} [W_i]_m, \qquad [W_i]_m = [P]^{-1}[T_i]_m[P]. \tag{7}$$

For an ordered bay the wave transfer matrix is diagonal, but for a disordered bay it is not, which means that there is reflection of the energy-carrying waves in the disordered system, and thus localization. The item of interest here is the (1,1) element of $[\mathscr{W}_N]_m$, which is the ratio of the incident to the transmitted wave amplitude for the N-bay disordered segment. This leads to the rate of decay per bay, or the localization factor (see Appendix):

$$\gamma_m = \lim_{N \to \infty} \frac{1}{N} \ln |[\mathscr{W}_N]_{m(1,1)}|. \tag{8}$$

The problem presented by this approach is that $[W_i]_m$ is a random matrix, and therefore $[\mathscr{W}_N]_m$ cannot be strictly evaluated as N goes to infinity. This obstacle can be overcome by approximating $[W_i]_m$ using perturbation techniques, and extracting the first order terms of the product of the wave transfer matrices. We thus have a first order approximation of $[\mathscr{W}_N]_{m(1,1)}$. We can then apply equation (8) to find the localization factor.

In order to apply perturbation techniques, two cases must be considered. The first is that of strong coupling (small mistuning-to-coupling ratio), $\sigma/R \ll 1$. Since $(\Delta f_i)/R$ is small compared to the other terms, this can be considered a perturbation. Thus, $[T_i]_m$ can be expanded as

$$[T_i]_m = \begin{bmatrix} \dfrac{1+2R-\bar{\omega}^2}{R} & -1 \\ 1 & 0 \end{bmatrix} + \begin{bmatrix} \dfrac{\Delta f_i}{R} & 0 \\ 0 & 0 \end{bmatrix} = [T_0] + [\Delta T_i]_m. \tag{9}$$

This is a classical perturbation technique, since disorder is considered to be a perturbation of the ordered system. Next, the matrices are transformed:

$$[W_i]_m = [P]^{-1}([T_0] + [\Delta T_i]_m)[P] = [W_0] + [P]^{-1}[\Delta T_i]_m[P]. \tag{10}$$

Taking the first order terms of the product shown in equation (7) yields

$$[\mathscr{W}_N]_m \approx [W_0]^N + \sum_{l=1}^{N} [W_0]^{l-1}[P]^{-1}[\Delta T_{N-l+1}]_m[P][W_0]^{N-l}. \tag{11}$$

Using equation (8), the approximate localization factor is found to be

$$\gamma_m \approx \frac{\sigma^2}{2(\bar{\omega}^2-1)(1+4R-\bar{\omega}^2)}, \qquad \sigma/R \ll 1. \tag{12}$$

Note that this approximation is valid only in the passband ($1 < \bar{\omega}^2 < 1+4R$). Furthermore, it fails near the passband edges.

The second case to be considered is that of weak coupling (large mistuning-to-coupling ratio), $\sigma/R \gg 1$. The classical perturbation technique is no longer valid. A modified perturbation technique must be used, where coupling is considered to be the disturbance. The expansion is thus

$$[T_i]_m = \begin{bmatrix} \dfrac{1+2R-\bar{\omega}+\Delta f_i}{R} & 0 \\ 0 & 0 \end{bmatrix} + \begin{bmatrix} 0 & -1 \\ 1 & 0 \end{bmatrix}. \tag{13}$$

Following the same methodology as for the weak mistuning case, the localization factor is

$$\gamma_m \approx -\ln R - 1 + \frac{1+2R-\bar{\omega}^2+W}{2W} \ln|1+2R-\bar{\omega}^2+W|$$

$$-\frac{1+2R-\bar{\omega}-W}{2W} \ln|1+2R-\bar{\omega}^2-W|, \qquad \sigma/R \gg 1. \tag{14}$$

The localization factors for representative strongly and weakly coupled systems are shown in Figure 3 as a function of $\bar{\omega}^2$ (for a more complete treatment of the mistuned–undamped system, see reference [16]).

It is important to understand, however, that these localization factors are ensemble-averaged values for the rate of spatial amplitude decay of the chain of oscillators. A single realization of a finite disordered system may show behavior which is quite different from this expected decay. This idea will be discussed further in section 4.3.

3. THE TUNED–DAMPED SYSTEM

3.1. THE PROPAGATION CONSTANT

We now introduce damping into the original (tuned) model by considering each beam to have uniform structural damping. The coupling springs are still considered to be undamped. The choice of structural damping is appropriate since the model represents an engineering structure excited by a harmonic force input. This damping adds an imaginary term to the equations of motion. If we express these equations in state vector form, the displacement transfer matrix becomes

$$[T]_d = \begin{bmatrix} \dfrac{1 + 2R - \bar{\omega}^2 + j\delta}{R} & -1 \\ 1 & 0 \end{bmatrix}, \tag{15}$$

where $j = \sqrt{-1}$, δ is the structural damping factor, and the subscript d denotes a damped system.

Note that since the damping is considered to be identical for all oscillators, so is the associated transfer matrix. This allows us to find an exact formula for the exponential decay constant for the tuned–damped system, which is simply the real part of the propagation constant [17]. Recalling that $\gamma = \ln|\lambda_1|$, where λ_1 is the eigenvalue of the transfer matrix of modulus greater than or equal to one, we find:

$$\gamma_d = \ln|(1/2R)[1 + 2R - \bar{\omega}^2 + j\delta \pm \sqrt{(1 - \bar{\omega}^2 + j\delta)(1 + 4R - \bar{\omega}^2 + j\delta)}]|. \tag{16}$$

Again, the radical is either added or subtracted in order to retrieve the largest eigenvalue. Note that equation (16) reduces to equation (5) for $\delta = 0$. The exponential decay constant is shown *vs.* $\bar{\omega}^2$ in Figure 4 for various values of damping.

We can express equation (16) in an alternate form by introducing the variable for passband position, α, which is defined as

$$\bar{\omega}^2 = 1 + \alpha R \tag{17}$$

such that the passband for the tuned–undamped system corresponds to $0 \leqslant \alpha \leqslant 4$. Therefore, α is a convenient variable for expressing the frequency in terms of its location

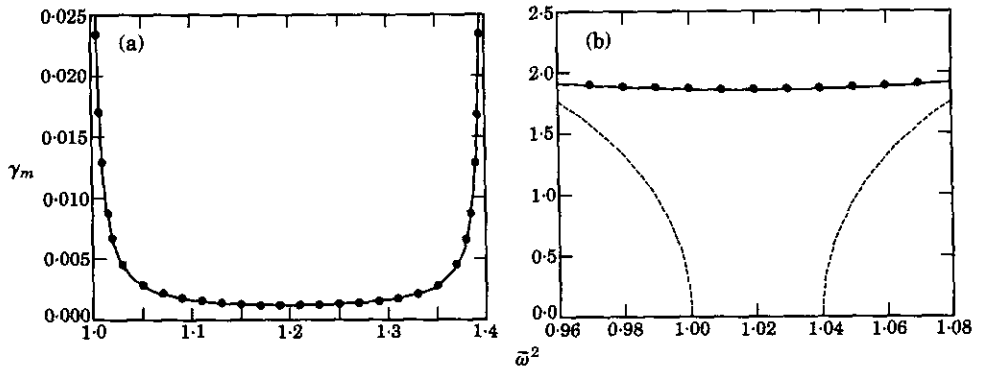

Figure 3. (a) Strong coupling perturbation (——) and Monte Carlo (●) results for the localization factor for a system with $R = 0{\cdot}1$, $\sigma/R = 0{\cdot}1$. Results are only shown within the passband, since the strong coupling perturbation results are not valid outside the passband. (b) Weak coupling perturbation (——) and Monte Carlo (●) results for the localization factor for a system with $R = 0{\cdot}01$, $\sigma/R = 10$. The decay constant (-------) for the tuned system is also shown.

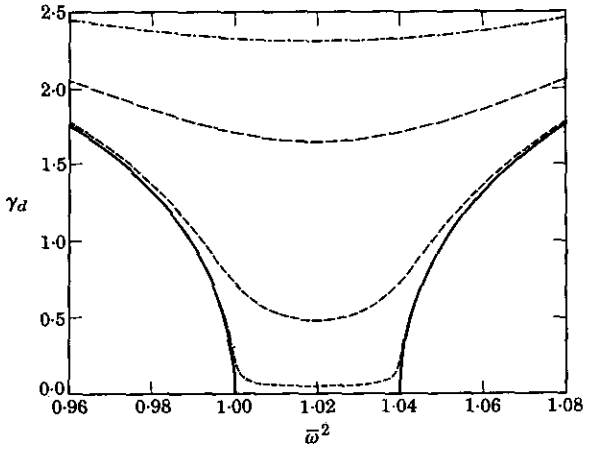

Figure 4. The real part of the propagation constant for a tuned–damped system with $R = 0{\cdot}01$, shown for various values of damping: $\delta/R = 10$ (—·—·), 5 (— — —), 1 (– – –), 0·1 (·····) and 0 (——).

relative to this passband. Substituting equation (17) into equation (16), we find that

$$\gamma_d = \ln|\tfrac{1}{2}[(2-\alpha)+\mathrm{j}(\delta/R) \pm \sqrt{(-\alpha+\mathrm{j}\delta/R)((4-\alpha)+\mathrm{j}\delta/R)}]|. \tag{18}$$

Hence the magnitude of the real part of the propagation constant depends on the damping-to-coupling ratio, δ/R, just as the localization factor depends on σ/R.

Simplified forms of equations (16) and (18) may be found in the cases of strong and weak coupling. For the case of strong coupling, we simplify equation (16), using the fact that δ/R is small compared to the other terms. After some algebra, it can be shown that

$$\gamma_d \approx \delta/\sqrt{(\bar{\omega}^2-1)(1+4R-\bar{\omega}^2)}, \qquad \delta/R \ll 1; \tag{19}$$

or, using passband position,

$$\gamma_d \approx \frac{1}{\sqrt{\alpha(4-\alpha)}}\frac{\delta}{R}, \qquad \delta/R \ll 1. \tag{20}$$

This expression is only valid inside the passband.

For the case of weak coupling, we expand equations (16) and (18) for large values of δ/R. After some algebra, this yields

$$\gamma_d \approx \tfrac{1}{2}\ln[((1+2R-\bar{\omega}^2)/R)^2+(\delta/R)^2], \qquad \delta/R \gg 1; \tag{21}$$

or,

$$\gamma_d \approx \tfrac{1}{2}\ln[(2-\alpha)^2+(\delta/R)^2], \qquad \delta/R \gg 1. \tag{22}$$

From the above equations, we can see that while structural damping appears in the equations of motion as a complex stiffness whose magnitude does not depend on frequency, the spatial decay rate in the periodic system due to structural damping is nevertheless frequency dependent. Furthermore, from Figure 4 and equations (20) and (22), we note that the exponential decay rate increases with damping, linearly for strong coupling and logarithmically for weak coupling. This dependence is similar to that of the localization factor on coupling. Finally, γ_d is minimum at mid-passband, and increases away from mid-passband, similar to the localization factor.

3.2. DYNAMIC RESPONSE OF THE TUNED–DAMPED SYSTEM

In order better to understand the behavior of the tuned–damped system, we now examine the frequency response of individual oscillators in the system. This is done by first writing the equations of motion in matrix form, with damping included:

$$\begin{bmatrix} \Upsilon & -R & 0 & \cdots & 0 \\ -R & \ddots & \ddots & \ddots & \vdots \\ 0 & \ddots & \ddots & \ddots & 0 \\ \vdots & \ddots & \ddots & \ddots & -R \\ 0 & \cdots & 0 & -R & \Upsilon \end{bmatrix} \begin{bmatrix} u_1/\bar{F} \\ \vdots \\ \vdots \\ \vdots \\ u_n/\bar{F} \end{bmatrix} = \begin{bmatrix} 1 \\ 0 \\ \vdots \\ \vdots \\ 0 \end{bmatrix}, \tag{23}$$

where $\Upsilon = 1 + 2R - \bar{\omega}^2 + j\delta$. The system matrix in equation (23) will be referred to as $[A]$, and the right side vector will be called **b**.

This system of equations can be solved by applying Cramer's rule, which states that the ith unknown variable, $u_i/\bar{F}$, is the determinant of $[A]$ with the ith column replaced by **b**, divided by the determinant of $[A]$. The determinant in the numerator of this expression follows a recursive relationship, and can be restated to obtain

$$\frac{u_i}{\bar{F}} = R^{i-1} \frac{\det([A] \text{ with first } i \text{ rows and columns removed})}{\det[A]}. \tag{24}$$

The determinant of these matrices can be found by diagonalizing them and taking the product of the diagonal terms. Equation (24) becomes

$$\frac{u_i}{\bar{F}} = R^{i-1} \frac{\Pi_{r=1}^{N-i}((\bar{\omega}_r)_{N-i}^2 - \bar{\omega}^2 + j\delta)}{\Pi_{r=1}^{N}((\bar{\omega}_r)_N^2 - \bar{\omega}^2 + j\delta)}, \tag{25}$$

where $(\bar{\omega}_r)_{N-i}$ and $(\bar{\omega}_r)_N$ are the rth natural frequencies for the tuned–undamped chains with $N-i$ and N degrees of freedom, respectively. Inspection of the denominator reveals that the resonant frequencies of the structurally damped system are the same as those of the undamped system.

The natural frequencies of the undamped system have been shown to be [19]:

$$(\bar{\omega}_r)_N^2 = 1 + 2R(1 - \cos r\pi/(N+1)), \qquad r = 1, \ldots, N. \tag{26}$$

Substituting this expression into equation (25), and restating the input frequency in terms of passband position α, we obtain

$$\frac{u_i}{\bar{F}} = \frac{1}{R} \frac{\Pi_{r=1}^{N-i}(2(1 - \cos r\pi/(N-i+1)) - \alpha + j\delta/R)}{\Pi_{r=1}^{N}(2(1 - \cos r\pi/(N+1)) - \alpha + j\delta/R)}, \qquad i = 1, \ldots, N. \tag{27}$$

Note that u_i/F depends on N, the number of oscillators in the system. It is important to recall, however, that we are primarily interested in the dynamics of the infinite system.

Numerically, we have found that if N is large enough, an oscillator responds as if it were part of a semi-infinite system. In other words, increasing the size of the system does not affect that oscillator's response to the harmonic excitation because the right-end boundary effects become negligible. When this occurs, we say that the oscillator exhibits *infinite behavior*. The minimum number of oscillators required to achieve infinite behavior (within some accuracy) across the entire passband for a single oscillator depends on the damping-to-coupling ratio. If δ/R is large, the excitation source energy is greatly dissipated and the boundary at the right end has little effect on the system's response, even for a system consisting of only a few oscillators. If δ/R is small,

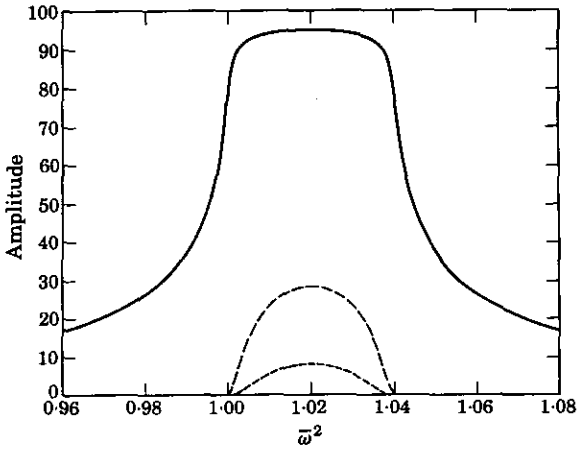

Figure 5. The vibration amplitude of the first (——), 25th (– – –) and 50th (- - - - -) oscillators of a 100-oscillator tuned–damped system; $R = 0{\cdot}01$, $\delta/R = 0{\cdot}1$.

the dissipation is more gradual along the chain, and thousands of oscillators may be required to eliminate the boundary effects. In general, we consider a system to be exhibiting infinite behavior if the decay rate due to damping is within 0·1% of the real part of the theoretical propagation constant for the infinite system (equation (16)). For undamped–mistuned systems, right-end boundary effects are negligible if N is chosen such that it is much greater than the localization length scale $1/\gamma$ (on a per bay basis) [16].

Once we have achieved infinite behavior for the entire system, we can look at the frequency response of any oscillator as if it were part of a semi-infinite chain. We now examine the comparative response of various oscillators in a tuned-damped chain, as shown in Figure 5. The first oscillator shows a somewhat squared peak, and near the passband edges the amplitude decreases significantly, but does not become vanishingly small. The response of the 25th oscillator, however, shows a much smaller and more rounded peak, and a more dramatic decrease in amplitude at frequencies near the passband edges. The response of the 50th oscillator follows the same trend: the peak is even smaller, and the response becomes vanishingly small at frequencies just inside the passband. This behavior follows directly from the fact that γ_d is larger near the edges of the passband, and minimum at mid-passband. Therefore, at mid-passband the energy from the excitation source passes through the system more freely than at other frequencies. At these other frequencies, the spatial decay is greater, and the further the frequency is from mid-passband, the stronger the decay.

Now let us remove the *left-end* boundary effects. We can do this by temporarily changing our excitation scheme so that we are exciting at the middle of the usual tuned–damped chain of oscillators. We consider a 1000-oscillator chain excited at the 500th oscillator, with $R = 0{\cdot}01$ and $\delta/R = 0{\cdot}1$. The parameters were chosen so that the oscillators respond as if they were part of an infinite (as opposed to semi-infinite) tuned–damped chain. In Figure 6 are shown the responses of the 500th, 505th, 515th, and 525th oscillators in this system. Note that the 500th (driven) oscillator now has a double-peaked response, with one crest occurrring at each edge of the passband. The response of the 505th oscillator exhibits a similar double peak, although the response is sharply attenuated outside of the passband as we would expect. The response of the 515th oscillator, however, does not show two obvious

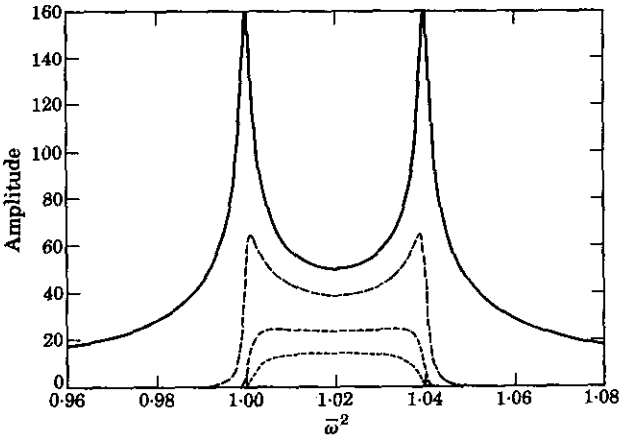

Figure 6. The vibration amplitude of the 500th (——), 505th (— —), 515th (– – –) and 525th (- - - -) oscillators of a 1000-oscillator tuned–damped system excited at the 500th oscillator; $R = 0{\cdot}01$, $\delta/R = 0{\cdot}1$.

peaks because, as discussed for Figure 5; the spatial decay due to damping is greater near the passband edges than at mid-passband. Finally, the 525th oscillator's response shows only a single peak, with the response becoming vanishingly small at the passband edges.

3.3. EQUIVALENT DAMPING DUE TO DISORDER

It should be emphasized that the expression for γ_d in equation (16) is exact, since the transfer matrix for the tuned–damped system is identical for all bays. This differs from the mistuned–undamped system, which is characterized by random disorder at each bay, and therefore by random transfer matrices.

This contrast reflects the differences in the physical mechanisms of decay for the two systems. The tuned–damped system dissipates the excitation energy. This dissipation occurs in the same manner at each bay, so the decay is uniform along the chain. The mistuned–undamped system, however, scatters the excitation energy. Each oscillator reflects some of the incident energy and transmits the rest, and because of the randomness of the disorder, the scattering is not identical for all oscillators. However, for the *typical* case, the system will show a spatial decay of vibration amplitude along the chain. When ensemble-averaged (or, equivalently, asymptotically), this decay rate is exponential [6].

We now attempt to determine how the magnitude of these decay rates compare; or, alternatively, we can compare the relative magnitudes of damping and disorder, given that the decay rates are equivalent. This leads us to the concept of *equivalent damping*—the value of damping, in terms of the standard deviation of disorder, σ, which would give rise to the same decay rate in the damped system as σ would in the mistuned system. Again, we emphasize the fact that disorder leads to a spatial amplitude decay by confining—or localizing—the excitation energy, while damping dissipates the excitation energy. By comparing spatial amplitude decay rates we do not mean to say that a certain amount of disorder affects a system in an identical manner as does damping, and the term "equivalent damping" should not be construed as implying that the two mechanisms are equivalent. Rather, we are interested in determining the relative magnitude of disorder needed to produce the spatial amplitude decay more commonly associated with damping effects.

We can find the equivalent damping δ_{eq} for the cases of strong and weak coupling. First, for strong coupling the approximate decay rates, γ_m and γ_d, are given by equations (12) and (19). Setting these two expressions to be equivalent, we find that

$$\delta_{eq} = \frac{\sigma^2}{2\sqrt{(\bar{\omega}^2 - 1)(1 + 4R - \bar{\omega}^2)}}, \qquad \sigma/R \quad \text{and} \quad \delta/R \ll 1; \tag{28}$$

or, in terms of passband position,

$$\delta_{eq} = \frac{\sigma^2}{2R\sqrt{\alpha(4 - \alpha)}}, \qquad \sigma/R \quad \text{and} \quad \delta/R \ll 1. \tag{29}$$

This expression is valid only in the passband ($0 < \alpha < 4$). Note that the equivalent damping is minimum at mid-passband and increases as the frequency approaches the passband edges.

Next, we consider the case of weak coupling. Unfortunately, for this case the calculation of δ_{eq} is not as straightforward, and we are unable to retrieve a simple form of the general expression of equivalent damping. We therefore choose to evaluate the equivalent damping at mid-passband only. This yields an expression which can be readily analyzed. In addition, there is little change in the value of the real part of the propagation constant with respect to frequency for weak coupling (see Figures 3 and 4), so the mid-passband value is a good estimate of γ_d throughout the passband. Evaluating equations (14) and (21) at mid-passband, we find the equivalent damping at mid-passband to be

$$\delta_{eq}^{mid} = (\sqrt{3}/\mathrm{e})\sigma, \qquad \sigma/R \quad \text{and} \quad \delta/R \gg 1. \tag{30}$$

Note that for weak coupling the equivalent damping is proportional to σ, a first order effect of disorder; but for strong coupling, the equivalent damping is proportional to σ^2, a second order effect. This means that for weak coupling, disorder yields relatively large equivalent damping, and the effects of damping and mistuning on the spatial amplitude decay rate are comparable. This could have an impact on vibration attenuation, especially in lightly damped structures. However, for a system with strong coupling, disorder provides little equivalent damping, and the effects of damping dominate. This suggests that weak localization is of little interest to the structural dynamicist.

4. THE MISTUNED–DAMPED SYSTEM

4.1. THE DAMPED LOCALIZATION FACTOR

We now proceed to analyze a system which has *both* mistuning *and* structural damping. In particular, we would like to find out how disorder and damping contribute to the overall spatial decay in the system. In order to do this, we must find an expression for the (average) exponential decay constant for the mistuned–damped system. We shall refer to this decay constant as the *damped localization factor*.

The displacement transfer matrix for this system includes both a disorder and a damping term:

$$[T_i]_{md} = \begin{bmatrix} \dfrac{1 + 2R - \bar{\omega}^2 + \Delta f_i + \mathrm{j}\delta}{R} & -1 \\ 1 & 0 \end{bmatrix}, \tag{31}$$

where the subscript *md* denotes the mistuned and damped system. Since the mistuning term is a random variable, we are unable to find an exact expression for the damped localization factor. Therefore, we must use stochastic perturbation techniques in order to

find approximations in the cases of strong and weak coupling, just as we did for the mistuned–undamped system in section 2.2.

4.1.1. *Strong coupling*

Here, we treat both mistuning and damping as perturbations in the transfer matrix. Accordingly, we require that *both* the mistuning-to-coupling *and* the damping-to-coupling ratio be small.

We first separate the transfer matrix into unperturbed and perturbation matrices:

$$[T_i]_{md} = [T_0] + [\Delta T_i]_m + [\Delta T]_d$$
$$= \begin{bmatrix} \dfrac{1+2R-\bar{\omega}^2}{R} & -1 \\ 1 & 0 \end{bmatrix} + \begin{bmatrix} \dfrac{\Delta f_i}{R} & 0 \\ 0 & 0 \end{bmatrix} + \begin{bmatrix} \dfrac{j\delta}{R} & 0 \\ 0 & 0 \end{bmatrix}. \tag{32}$$

We then perform a co-ordinate transformation in order to obtain the wave transfer matrix $[W_i]$. The transformation matrix $[P]$ is the matrix of eigenvectors of $[T_0]$. For frequencies in the passband, it is of the form

$$[P] = \begin{bmatrix} 1 & 1 \\ e^{-jk} & e^{jk} \end{bmatrix}, \tag{33}$$

where k is the wavenumber, defined by the dispersion relation [16] as $\bar{\omega}^2 = 1 + 4R \sin^2(k/2)$.

Next, we take a first order approximation of the overall wave transfer matrix, which is the product from N to 1 of the individual wave transfer matrices. Using a modified form of equation (11), this leads to the first order approximation of the (1,1) element:

$$([\mathscr{W}_N]_{md})_{(1,1)} \approx e^{jkN} + (e^{jkN}/2R \sin k) \sum_{i=1}^{N} (\delta - j\Delta f_i). \tag{34}$$

We can now proceed to find the damped localization factor, which is (see the Appendix)

$$\gamma_{md} = \langle (1/N) \ln |([\mathscr{W}_N]_{md})_{(1,1)}| \rangle, \tag{35}$$

where $\langle\ \rangle$ denotes an average or expected value. Replacing the wavenumber with the input frequency and solving yields

$$\gamma_{md} \approx \frac{\delta}{\sqrt{(\bar{\omega}^2-1)(1+4R-\bar{\omega}^2)}} + \frac{\sigma^2}{2(\bar{\omega}^2-1)(1+4R-\bar{\omega}^2)}, \qquad \sigma/R \quad \text{and} \quad \delta/R \ll 1, \tag{36}$$

which is a summation of the strong coupling approximations for the tuned–damped and mistuned–undamped systems. For strong coupling, the two decay rates simply add up.

If we now state the damped localization factor in terms of passband position, we find

$$\gamma_{md} \approx \frac{1}{\sqrt{\alpha(4-\alpha)}}\left(\frac{\delta}{R}\right) + \frac{1}{2\alpha(4-\alpha)}\left(\frac{\sigma}{R}\right)^2, \qquad \sigma/R \quad \text{and} \quad \delta/R \ll 1. \tag{37}$$

As with the strong coupling approximations in previous sections, this approximation is only valid inside the passband, and it fails near the passband edges. We should also note that the damping-to-coupling ratio appears as a first order term, while the mistuning-to-coupling ratio appears as a second order term. Since this approximation requires that both ratios be small, we can easily see that localization due to disorder has little effect on the

overall decay. For the strong coupling case, with disorder and damping of the same order of magnitude, the damping effects dominate.

4.1.2. *Weak coupling*

For this case, the coupling is considered to be a perturbation. From a simple inspection of the displacement transfer matrix, we can see that this is appropriate if coupling is small compared to *either* mistuning *or* damping. Therefore, for the weak coupling case, we require only that $\sigma/R \gg 1$ or $\delta/R \gg 1$. The transfer matrix is accordingly separated into unperturbed and perturbation matrices:

$$[T_i]_{md} = [T_{io}]_{md} + [\Delta T] = \begin{bmatrix} \dfrac{1 + 2R - \bar{\omega}^2 + \Delta f_i + j\delta}{R} & 0 \\ 0 & 0 \end{bmatrix} + \begin{bmatrix} 0 & -1 \\ 1 & 0 \end{bmatrix}. \tag{38}$$

The unperturbed matrix is diagonal, so no co-ordinate transformation is necessary to obtain the local wave transfer matrices. The first order approximation of the global wave transfer matrix is therefore:

$$[\mathscr{W}_N]_{md} \approx \prod_{i=N}^{1} [T_{io}]_{md} + \sum_{l=1}^{N} \left[\left(\prod_{i=N}^{l+1} [T_{io}]_{md} \right) [\Delta T] \left(\prod_{i=l-1}^{1} [T_{io}]_{md} \right) \right]. \tag{39}$$

Noting that the (1,1) element of the sum in equation (39) is zero, we obtain

$$([\mathscr{W}_N]_{md})_{(1,1)} \approx \prod_{i=N}^{1} \left(\frac{1 + 2R - \bar{\omega}^2 + \Delta f_i + j\delta}{R} \right). \tag{40}$$

As before, we need to take the ensemble-average of the natural logarithm of the modulus of this element in order to retrieve the damped localization factor. After some manipulations, we obtain

$$\gamma_{md} \approx -\ln R + (1/4W) \int_{-W}^{W} \ln [(1 + 2R - \bar{\omega}^2 + x)^2 + \delta^2] \, dx, \tag{41}$$

where W $(=\sqrt{3}\sigma)$ is the half-width of the uniform distribution. Finally, evaluation of the integral yields the general expression for the damped localization factor for weak coupling:

$$\begin{aligned} \gamma_{md} \approx & -1 + \frac{1 + 2R - \bar{\omega}^2 + W}{4W} \ln \left(\left(\frac{1 + 2R - \bar{\omega}^2 + W}{R} \right)^2 + \left(\frac{\delta}{R} \right)^2 \right) \\ & - \frac{1 + 2R - \bar{\omega}^2 - W}{4W} \ln \left(\left(\frac{1 + 2R - \bar{\omega}^2 - W}{R} \right)^2 + \left(\frac{\delta}{R} \right)^2 \right) \\ & + \frac{\delta}{2W} \arctan \left(\frac{1 + 2R - \bar{\omega}^2 + W}{\delta} \right) \\ & - \frac{\delta}{2W} \arctan \left(\frac{1 + 2R - \bar{\omega}^2 - W}{\delta} \right), \qquad \frac{\sigma}{R} \text{ or } \frac{\delta}{R} \gg 1. \end{aligned} \tag{42}$$

Putting equation (42) in terms of passband position α, we obtain simply

$$\begin{aligned} \gamma_{md} \approx & -1 + \tfrac{1}{4}((R/W)(2 - \alpha) + 1) \ln ((2 - \alpha + W/R)^2 + (\delta/R)^2) \\ & - \tfrac{1}{4}((R/W)(2 - \alpha) - 1) \ln ((2 - \alpha - W/R)^2 + (\delta/R)^2) \\ & + (\delta/2W) \arctan ((R/\delta)(2 - \alpha) + W/\delta) \\ & - (\delta/2W) \arctan ((R/\delta)(2 - \alpha) - W/\delta), \qquad \sigma/R \text{ or } \delta/R \gg 1. \end{aligned} \tag{43}$$

We observe that these approximations are in part a function of the mistuning-to-coupling ratio σ/R, and the damping-to-coupling ratio δ/R. The effect of these parameters on γ_{md} is discussed in section 4.2.

4.2. PERTURBATION METHOD AND MONTE CARLO RESULTS

Here, we compare the analytical expressions for the damped localization factor—equations (36) and (42)—with the values obtained by Monte Carlo simulations. The Monte Carlo results consist of the ensemble-averaged numerical solution to the problem $[A(\bar{\omega}^2)]\mathbf{u} = \mathbf{b}$, where $[A(\bar{\omega}^2)]$ is the system matrix of equation (23) with disorder added, $\mathbf{u}$ is the vector of non-dimensionalized vibration amplitudes, and $\mathbf{b}$ is the non-dimensionalized forcing vector. $[A(\bar{\omega}^2)]$ contains a random mistuning term which was assigned by a random number generator for each of many realizations. This problem was solved in each realization by numerically inverting the complex matrix $[A(\bar{\omega}^2)]$, and pre-multiplying $\mathbf{b}$ by this inverse. The numerical accuracy of this procedure was examined by solving several tuned–damped systems, for which exact solutions exist. The numerical precision was found to be of an order of magnitude which is well within that needed for graphical comparison with the analytical results. Once the response of the system was solved, the logarithms of the moduli of the amplitudes were taken. A least-squares technique was used to find the slope of these log distributions. The damped localization factor was then calculated as the negative of the slope. This result was ensemble-averaged over many realizations of disordered systems, in order to determine an estimate of the damped localization factor.

The number of bays for the system was chosen to be close to the maximum number which would yield numerically stable results for the given parameters. This number ranged from 30 for systems with weak coupling to 8500 for systems with strong coupling. In all cases, the chain length was sufficient to ensure that the right-end boundary effects were negligible. The number of realizations for each data point were then chosen so as to allow the averaged damped localization factor to converge to a value which did not significantly change with further iterations. Typically, 5000 iterations were needed for systems with large or moderate disorder-to-coupling ratio.

Perturbation and Monte Carlo results for the strong coupling case of the mistuned–damped system are displayed in Figure 7. Results are shown for the frequency range located within the passband of the tuned–undamped system, because—as noted earlier—the perturbation approximation fails at the passband edges. Consequently, we see good agreement between the two results for most of the passband, but the perturbation results diverge from the Monte Carlo results near the passband edges. The perturbation approximations for the localization factor of the mistuned–undamped system (γ_m) and for the real part of the propagation constant of the tuned–damped system (γ_d) are also shown. Recall that for strong coupling, the approximation for the damped localization factor was found to be the sum of these two results. It is easy to see that when the mistuning-to-coupling and the damping-to-coupling ratio are of similar magnitude, the effects of mistuning are very small compared to those of damping. This is predicted by equation (28), which shows that the equivalent damping for strong coupling is proportional to the square of the mistuning.

Perturbation and Monte Carlo results for the damped localization factor for the case of weak coupling are shown in Figure 8. Here, γ_{md} is *not* the sum of γ_m and γ_d. The effects of damping and disorder exhibit a more complicated interaction for weak coupling. Note that the disorder makes a substantial contribution to the overall decay, as predicted by equation (30). In addition, the approximation for the damped localization factor

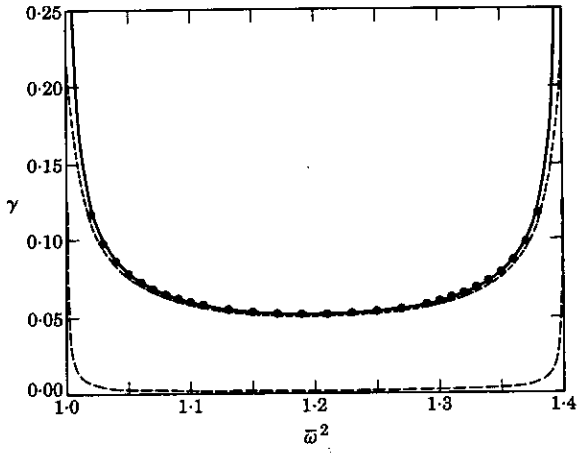

Figure 7. Strong coupling perturbation (——) and Monte Carlo (●) results for the damped localization factor of a system with $R = 0{\cdot}1$, $\delta/R = 0{\cdot}1$, $\sigma/R = 0{\cdot}1$. Also shown are γ_d (- - - -) for the system if $\sigma/R = 0$ (tuned–damped), and γ_m (— — —) for the system if $\delta/R = 0$ (mistuned–undamped).

remains valid outside of the passband, and shows good agreement with the Monte Carlo results.

Next, we consider the possibility that either the damping-to-coupling ratio or the mistuning-to-coupling ratio is large, and the other ratio is small. The approximate damped localization factor for $\sigma/R = 10$ and δ/R of various values is shown in Figure 9. The top curve is γ_{md} for $\delta/R = 10$. As δ/R is decreased to 1, γ_{md} exhibits a significant decrease in magnitude, but the approximation still shows good agreement with the Monte Carlo results. The approximation also holds for $\delta/R = 0{\cdot}1$ but, for this drop in damping, the decrease in magnitude of γ_{md} is not as great. Furthermore, γ_{md} for these parameters is almost the same as γ_m for the undamped system, shown by the solid line. Decreasing the damping further does not significantly change the value of γ_{md}, although it does approach γ_m. This shows that in the limit, as $\delta/R \to 0$, the perturbation results for γ_m and γ_{md} are equivalent.

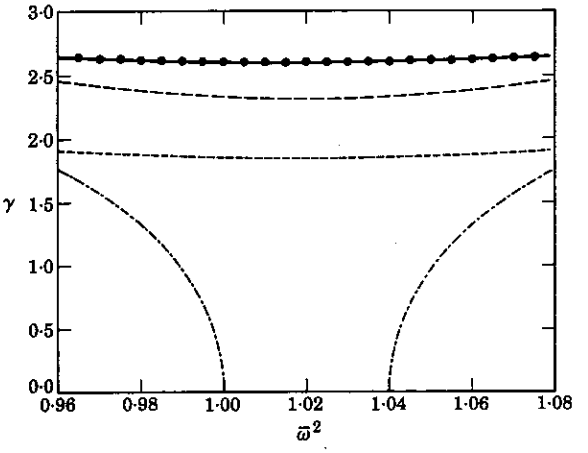

Figure 8. Weak coupling perturbation (——) and Monte Carlo (●) results for the damped localization factor of a system with $R = 0{\cdot}01$, $\delta/R = 10$, $\sigma/R = 10$. Also shown are γ_d (— — —) for the system if $\sigma/R = 0$, γ_m (- - - -) for the system if $\delta/R = 0$, and γ (— · — ·) for the system if $\sigma/R = 0$ and $\delta/R = 0$.

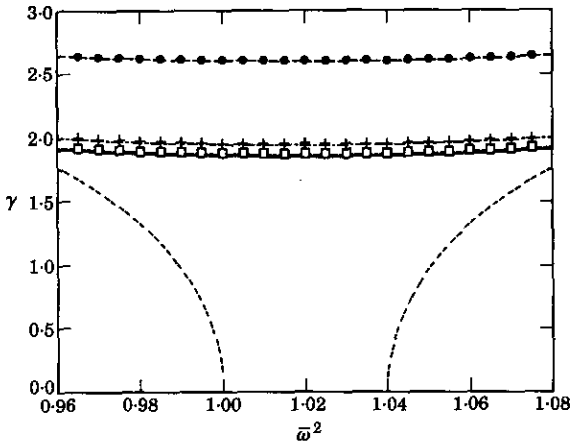

Figure 9. The effect of damping on the damped localization factor for a system with large disorder-to-coupling ratio, $R = 0{\cdot}01$, $\sigma/R = 10$. The following are shown: weak coupling perturbation (——) and Monte Carlo (●) results for $\delta/R = 10$; perturbation (— · — ·) and Monte Carlo (+) results for $\delta/R = 1$; and perturbation (- - - -) and Monte Carlo (□) results for $\delta/R = 0{\cdot}1$. Also shown are the weak coupling approximation for γ_m (——) for the system if $\delta/R = 0$, and γ (-- --) for the system if $\sigma/R = 0$ and $\delta/R = 0$. Note that γ_{md} for $\delta/R = 0{\cdot}1$ is almost equal to γ_m for $\delta/R = 0$.

The results for the case in which $\delta/R = 10$ and σ/R is decreased are shown in Figure 10. The top curve is again the damped localization factor for $\delta/R = 10$ and $\sigma/R = 10$. As we decrease the mistuning so that $\sigma/R = 1$, we note that there is a noticeable decrease in the magnitude of γ_{md}. However, the Monte Carlo results then seem to be coincident with γ_d for the tuned–damped system, shown as a solid line. Decreasing the value of σ/R further does not significantly affect γ_{md}. This leads to two conclusions. First, for the weak coupling case the effects of disorder vanish more quickly as σ/R is decreased than do the effects of damping as δ/R is decreased. Second, when mistuning approaches zero, γ_{md} approaches γ_d for the tuned–damped system. Also, both Figures 9 and 10 show that the approximations for the weak coupling remain valid as long as *either* the damping-to-

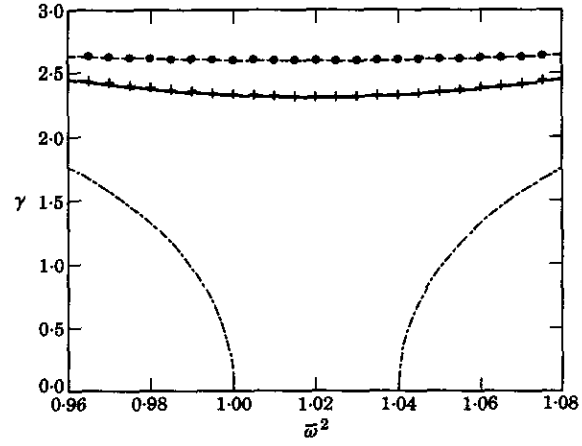

Figure 10. The effect of disorder on the damped localization factor for a system with large damping-to-coupling ratio, $R = 0{\cdot}01$, $\delta/R = 10$. The following are shown: weak coupling perturbation (——) and Monte Carlo (●) results for $\sigma/R = 10$; and Monte Carlo (+) results for $\sigma/R = 1$. Also shown are γ_d (——) for the system if $\sigma/R = 0$, and γ (— · — ·) for the system if $\sigma/R = 0$ and $\delta/R = 0$. The perturbation results for γ_{md} for $\sigma/R = 1$ are not included because they are coincident with γ_d shown.

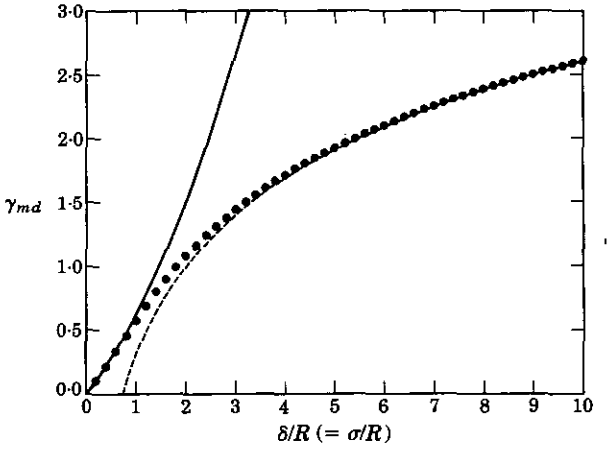

Figure 11. Strong coupling (——) and weak coupling (– – – –) perturbation results and Monte Carlo (●) results for the damped localization factor at the mid-passband frequency. The damped localization factor is shown for a range of values of δ/R, with σ/R held equal to δ/R.

coupling ratio *or* the mistuning-to-coupling ratio is large, as we reasoned in section 4.1.2. Furthermore, for the range of frequencies shown, the damped localization factor varies little in magnitude.

Finally, in Figure 11 is shown the relationship between the Monte Carlo results and the strong and weak coupling approximations at mid-passband. The decay constants are shown *vs.* the damping-to-coupling ratio (for $\delta/R = \sigma/R$). For strong coupling (small δ/R and σ/R), the Monte Carlo results are coincident with the weak decay approximation. As coupling decreases (these ratio approach a value of 1), the Monte Carlo results diverge from this approximation and smoothly approach the strong decay approximation. As δ/R and σ/R become large, the Monte Carlo and perturbation results coincide, and the variation of the damped localization factor becomes roughly logarithmic.

4.3. SINGLE REALIZATIONS OF MISTUNED–DAMPED SYSTEMS

So far we have investigated the interaction of damping and mistuning by formulating expressions for the damped localization factor which show quantitatively the role that each mechanism plays in the overall spatial amplitude decay of the system. This was verified by Monte Carlo simulations, in which the results of many realizations are averaged. Now let us look at some single realizations of the dynamic response of a mistuned–damped system, excited at its left end, so that we may gain a qualitative understanding of its behavior.

4.3.1. *Response of the chain of oscillators*

In Figure 12 is shown the forced response, to a left-end excitation, for one realization of a system with $\sigma/R = 0{\cdot}1$ and various values of damping. The input frequency was chosen so that it is approximately mid-way between two resonant frequencies. The response is shown on a natural log scale, so that exponential spatial amplitude decay will appear to be linear in these plots.

In plot (a), the system has $\delta/R = 0{\cdot}001$. The decay is therefore due largely to localization. The theoretical (Monte Carlo ensemble average) slope for spatial amplitude decay is shown as a dashed line (note that we are only interested in the slope of this line—the intercepts were arbitrarily chosen). The oscillator amplitudes follow a trend which roughly approximates this decay, but the individual responses are substantially scattered about the general

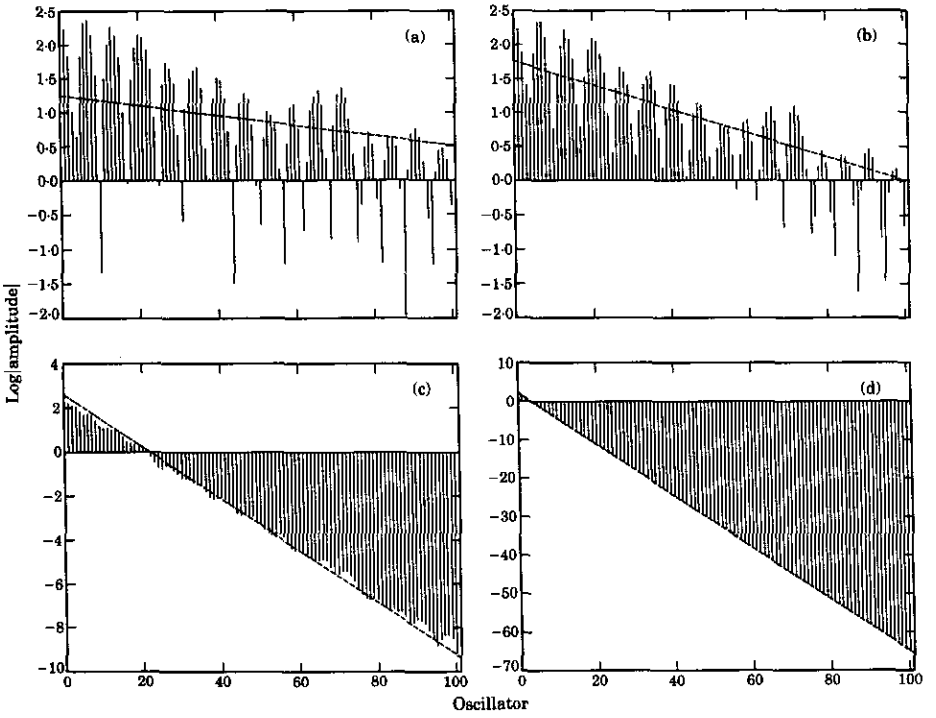

Figure 12. Vibration amplitudes (shown on a natural log scale to illustrate the rate of exponential decay) for a 100-oscillator mistuned–damped system; $R = 0{\cdot}1$, $\sigma/R = 0{\cdot}1$, $\bar{\omega}^2 = 1{\cdot}021$, and various values of δ/R. (a) $\delta/R = 0{\cdot}001$; (b) $\delta/R = 0{\cdot}01$; (c) $\delta/R = 0{\cdot}1$; (d) $\delta/R = 1$. In each case, the Monte Carlo averaged decay rate is portrayed by the slope of the line (- - - -) superimposed on the plot. Note that as damping is increased, the spatial decay becomes more uniform, approaching the averaged exponential decay rate.

trend. This agrees with the results of Hodges and Woodhouse [6]. In particular, there are a few oscillators which show a much smaller response than they would if the spatial amplitude decay were purely exponential. In plot (b), the damping is increased so that $\delta/R = 0{\cdot}01$. The response seems to follow the exponential trend more closely, and there are fewer radical deviations from this trend. In plot (c), damping is again increased to $\delta/R = 0{\cdot}1$, so now we have the condition $\delta/R = \sigma/R$. The response has been effectively smoothed out, and closely follows an exponential trend, although the rate of decay seems to differ slightly from the averaged rate. In plot (d), we increase damping to $\delta/R = 1$. Note that the spatial amplitude decay is now almost perfectly exponential, and corresponds to the averaged rate of decay. This illustrates that the decay caused by mistuning is only exponential asymptotically, and that individual realizations may feature large deviations from this average localization factor. On the other hand, damping yields an exactly exponential decay at each site.

4.3.2. *Right-end localization*

Since mode shapes can be localized about any oscillator, it is possible to see a response which shows large amplitudes at oscillators other than the driven oscillator. However, localized mode shapes have a small amplitude away from the localized region, so the further the localized part of the mode shape is from the excitation source, the less likely we are to excite that mode. Modes localized about the first few oscillators are easily excited by driving the first oscillator, and modes localized elsewhere are much more difficult to excite. Thus, when we ensemble-average the decay rate over many realizations of a

system, the atypical responses do not play a large role, and we retrieve the expected spatial decay rate—the localization factor [20].

The single realizations that we have examined so far for the mistuned–damped chain have shown localization near the driven oscillator, with a decay of spatial amplitude which is at least approximately exponential away from the driving source. We therefore have looked at what we might call typical responses. Although we have argued that localization far from the excitation source is rare, its striking nature dictates that we also examine such an atypical repsonse. We therefore consider the case of a mistuned–damped chain which exhibits localization at the right end of the chain, while the oscillators at the left (driven) end show little response. We will refer to this as *right-end localization.* In order to determine when and why this occurs, we must introduce the concept of modal amplitudes for the mistuned–damped system.

We begin by adding mistuning to the matrix $[A]$ of equation (23) so that $\Upsilon = 1 + 2R - \bar{\omega}^2 + \Delta f_i + j\delta$. If $[V]$ is the matrix of eigenvectors of this new $[A]$ matrix, then the vector of modal amplitudes (or normal co-ordinates), $\boldsymbol{\eta}$, is introduced by the following transformation:

$$\mathbf{u} = [V]\boldsymbol{\eta}. \tag{44}$$

Substituting this expression into equation (23), and pre-multiplying by $[V]^T$, leads to

$$[V]^T[A][V]\boldsymbol{\eta} = [V]^T \begin{bmatrix} 1 \\ 0 \\ \vdots \\ 0 \end{bmatrix}. \tag{45}$$

The matrix multiplication on the right side of this equation results in a column vector which is the first column of the matrix $[V]^T$. Since the columns of $[V]$ are the eigenvectors $\mathbf{v}_r$, the first column of its transpose consists of the first element of each eigenvector. Equation (45) becomes

$$\begin{bmatrix} \ddots & & 0 \\ & \bar{\omega}_r^2 - \bar{\omega}^2 + j\delta & \\ 0 & & \ddots \end{bmatrix} \boldsymbol{\eta} = \begin{bmatrix} \vdots \\ (\mathbf{v}_r)_1 \\ \vdots \end{bmatrix}, \qquad r = 1, \ldots, N. \tag{46}$$

Thus, the modulus of the rth modal amplitude is simply obtained as

$$|\boldsymbol{\eta}_r| = |(\mathbf{v}_r)_1| / \sqrt{(\bar{\omega}_r^2 - \bar{\omega}^2)^2 + \delta^2}, \qquad r = 1, \ldots, N, \tag{47}$$

where $\bar{\omega}_r$ is the rth natural frequency for the mistuned–undamped chain. This is the contribution of the rth mode shape to the amplitude of the total response of the system. Although we derived this equation for the mistuned–damped system, it is completely general.

For undamped systems, setting δ equal to zero in equation (47) would produce the correct expression for the rth modal amplitude. If we can excite the system at a frequency which is arbitrarily close to the rth resonant frequency, we can produce a response which is almost entirely in the rth mode (unless $(\mathbf{v}_r)_1 = 0$, in which case the rth mode is orthogonal to the excitation and therefore does not contribute to the forced response). For a damped system, the situation is different. From equation (47), we can see that the rth mode shape will dominate the response if

$$\frac{|(\mathbf{v}_r)_1|}{\sqrt{(\bar{\omega}_r^2 - \bar{\omega}^2)^2 + \delta^2}} \gg \frac{|(\mathbf{v}_i)_1|}{\sqrt{(\bar{\omega}_i^2 - \bar{\omega}^2)^2 + \delta^2}}, \qquad i = 1, \ldots, N, \quad i \neq r. \tag{48}$$

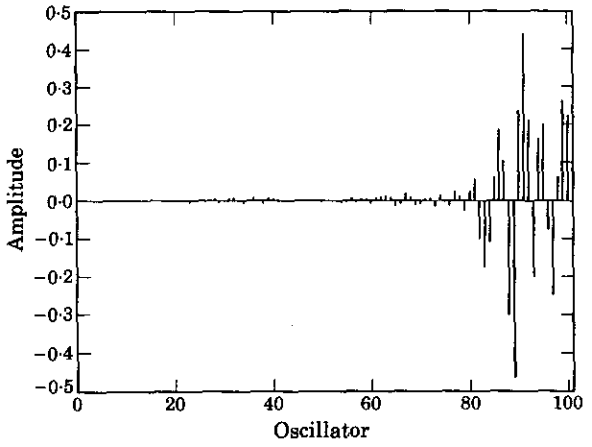

Figure 13. The 53rd mode shape of a 100-oscillator mistuned system; $R = 0{\cdot}01$, $\sigma/R = 1$.

The minimum value of the denominator on the left side is δ. This means that if damping is large enough, we will not be able to obtain a response which closely resembles the rth mode shape, unless its first component is large compared to the first components of the other mode shapes.

Now, let us examine an example of right-end localization. We consider a disordered system excited at the 53rd resonant frequency. The 53rd mode shape for this system is shown in Figure 13. It is clearly localized in a region near the right end of the system. The vibration amplitudes and modal amplitudes for various values of damping are shown in Figure 14. For sufficiently small damping, the response greatly resembles that mode shape. Thus, we see large amplitudes at the right end and small amplitudes toward the left end, despite the fact that this system is damped and disordered and is excited at the leftmost oscillator. As damping is increased, the requirement of equation (48) is no longer satisfied, and the response amplitude patterns are altered to resemble more closely the exponential spatial decay pattern which we would normally expect. For each response, the corresponding set of modal amplitudes is shown. Notice that the 53rd modal amplitude dominates for small damping, but it becomes small as damping increases, in which case the modes localized near the left end dominate.

Finally, we note that the localization factor describes the expected spatial decay rate for the oscillator amplitudes of a localized mode shape. As stated earlier, we can think of the spatial decay of the vibration amplitudes of the forced response as the result of an excitation of such localized modes. Without damping, we have seen that it is possible to excite any localized mode aribtrarily much. With damping, however, localization far from the excitation source is virtually eliminated.

4.3.3. *Frequency response of individual oscillators*

Now that we have observed the response of an entire chain, let us look at the frequency response of individual oscillators for a single realization of a mistuned–damped chain. We choose a system which has $\delta/R = 0{\cdot}5$, $\sigma/R = 1$ and consists of 100 oscillators. The frequency responses of the first and 25th oscillators are shown in Figure 15. The first oscillator features a response which is greater at lower frequencies in the passband, and has several peaks. This occurs because at certain frequencies, modes which are localized near this first oscillator are excited, and the response at the first oscillator is consequently greater near those frequencies. From our equations for the modal amplitudes of a

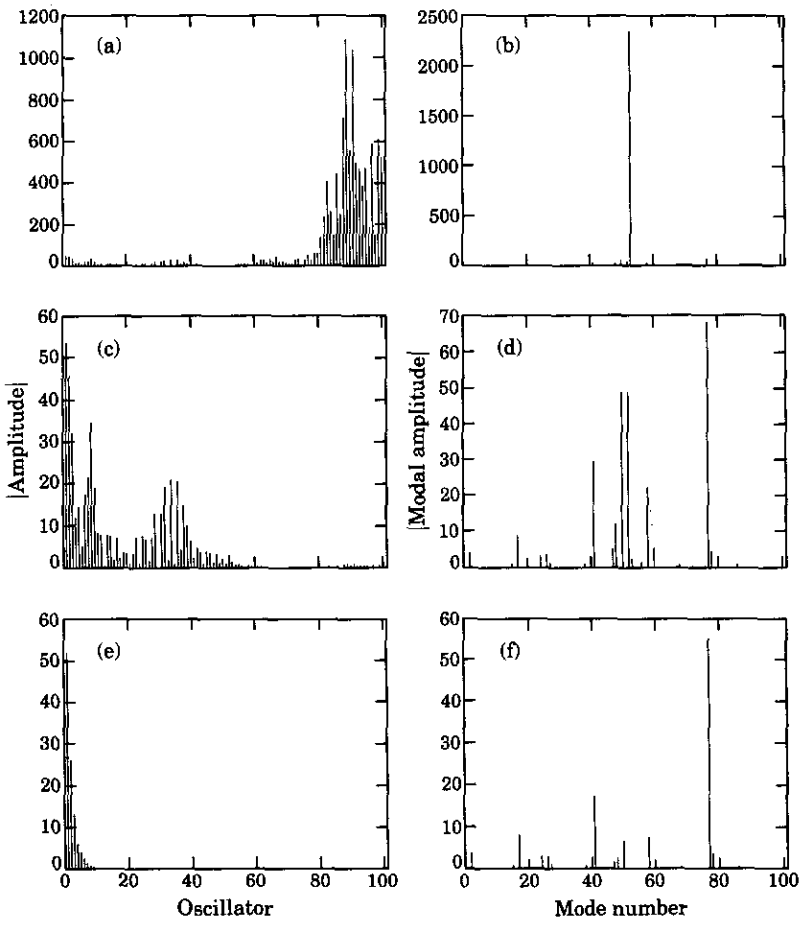

Figure 14. Vibration amplitudes and modal amplitudes for the mistuned system of Figure 13, excited at the 53rd natural frequency, with various values of δ/R: (a) vibration amplitudes for $\delta/R = 10^{-8}$; (b) modal amplitudes for $\delta/R = 10^{-8}$; (c) vibration amplitudes for $\delta/R = 10^{-5}$; (d) modal amplitudes for $\delta/R = 10^{-5}$; (e) vibration amplitudes for $\delta/R = 10^{-2}$; (f) modal amplitudes for $\delta/R = 10^{-2}$. For $\delta/R = 10^{-8}$, the system responds almost entirely in the 53rd mode, which is localized far from the excitation source. This is an example of right-end localization. As damping is increased, the expected spatial amplitude decay is observed. Note that even though the system is excited at the 53rd natural frequency, the damping must be extremely weak in order for right-end localization to occur.

mistuned–damped system, we know that if damping were increased, these peaks would be diminished, since the modal amplitudes would become less sensitive to the location of the input frequency. The frequency response for the first oscillator of a tuned chain with the same amount of damping is shown by a dashed line in Figure 15.

In addition to the fact that the response of the first oscillator of the mistuned chain features several peaks while the tuned response shows just one, there are two other differences. The first is that the maximum amplitude of the mistuned response does not occur at mid-passband. In fact, for this particular mistuning pattern, the peak response occurs near the edge of the passband, which most likely corresponds to a mode localized at the left end. Secondly, the mistuned oscillator shows a larger response than the tuned oscillator for much of the frequency range shown, but features a smaller response at other frequencies. These differences can be attributed to the nature of the spatial amplitude decay for the mistuned system. Disorder leads to a spatial amplitude decay because it causes the

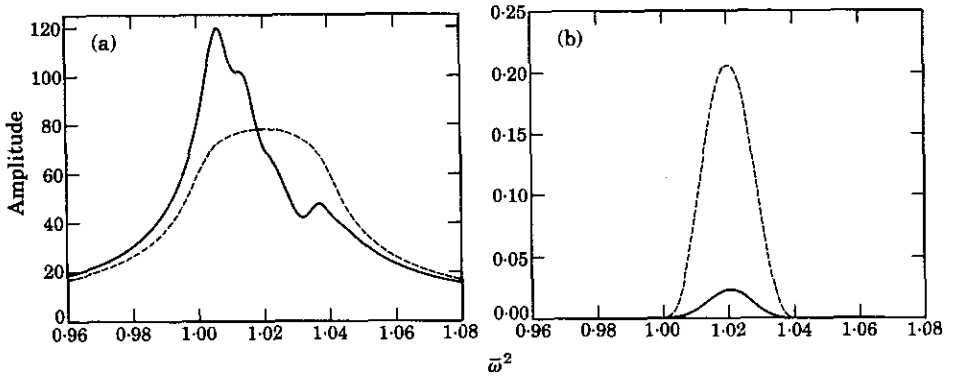

Figure 15. Vibration amplitudes for (a) the first oscillator and (b) the 25th oscillator of a 100-oscillator mistuned–damped system with $R = 0{\cdot}01$, $\delta/R = 0{\cdot}5$ and $\sigma/R = 1$ (——), shown *vs.* the vibration amplitudes for the same oscillators if $\sigma/R = 0$ (-----).

excitation energy to be partially reflected at each bay. Therefore, the energy tends to be confined near the excitation source of a mistuned system, and the first oscillator shows a greater response for most frequencies that it would in a tuned system. Furthermore, this reflection becomes more prevalent for frequencies away from mid-passband, as evidenced by the fact that the localization factor and damped localization factor are both minimum at mid-passband. Therefore, the mistuned system is likely to have a maximum response away from mid-passband. However, the random nature of mistuning dictates that for any given frequency, the excitation energy may be confined in a region away from the first oscillator. Therefore, for these frequencies, the first oscillator will show a smaller response than it would in a tuned system.

The response of the 25th oscillator in the mistuned–damped chain is remarkably different than that of the first. The shape of the frequency response now resembles that of a tuned system. However, if we compare the magnitude of this response to that of the tuned system, we see that the mistuned system's response is much smaller. We therefore observe the fundamental nature of spatial amplitude decay due to mistuning. The energy transmitted to the 25th oscillator has been attenuated, particularly near and outside the passband edges. Furthermore, this attenuation—although caused by a random scattering at each bay of the system—results in a smooth frequency response distribution, because the random effects of disorder have been spatially "averaged" by the influence of many bays. This supports the idea that the localization factor (damped or undamped) may be found either by taking the average of the decay rate of many finite systems, or by finding the amplitude decay of a system in an asymptotic sense, as the number of bays tends to infinity.

5. CONCLUSIONS

The effect of disorder and structural damping on the dynamics of a chain of coupled oscillators was examined. The disorder was considered to be a uniformly distributed random variable with a zero mean and standard deviation σ. The structural damping factor δ was taken to be the same for all oscillators. For a system with damping but no disorder, an exact expression was found for the exponential spatial decay constant γ_d. It was found to have a frequency dependence similar to that of the localization factor γ_m for a system with disorder but no damping. Thus, the vibration attenuation is minimal at the

mid-passband frequency, and increases as the frequency increases or decreases from this value.

The ensemble-averaged exponential decay constant for a mistuned–damped system is called the damped localization factor γ_{md}. This factor was found to depend on the damping-to-coupling ratio δ/R, the mistuning-to-coupling ratio σ/R, and the input frequency. Approximate expressions for γ_{md} were found for two cases: weak coupling, in which *either* δ/R *or* σ/R is large; and strong coupling, in which both ratio are small. For strong coupling, γ_{md} was shown to be a sum of the decay factors of the mistuned–undamped and the tuned–damped systems. Furthermore, when disorder and damping are of the same order of magnitude, disorder has little effect on the overall decay, and damping effects dominate. This means that localization effects are of little importance in strongly coupled systems. In the case of weak coupling, however, damping and disorder make comparable contributions to the damped localization factor. However, this factor is substantially less than the sum of the two individual decay rates.

Monte Carlo methods were used to obtain numerical approximations of the damped localization factor that supported the analytical expressions. In addition, the vibration amplitudes of the entire chain were found numerically for individual realizations of a mistuned–damped system with random disorder. It was observed that for a typical case, the spatial amplitude decay of the chain is only approximately exponential if σ/R is substantially larger than δ/R. However, if the magnitude of δ/R approaches or exceeds that of σ/R, then the chain will exhibit nearly uniform exponential decay. It was also shown that for certain *atypical* cases, it is possible to strongly excite a mode that is localized about an oscillator which is located far from the energy source, but this effect is virtually eliminated by even a small amount of damping.

ACKNOWLEDGMENTS

The work of the first author is supported by a National Science Foundation Graduate Research Fellowship. The work of the second author is supported by National Science Foundation Grant No. MSS-8913196. Dr Elbert L. Marsh is the grant monitor. The authors would also like to thank one of the referees for the very valuable comments regarding the double-peak response found when exciting the system at an intermediate oscillator.

REFERENCES

1. L. BRILLOUIN 1953 *Wave Propagation in Periodic Structures*. New York: Dover, second edition.
2. D. J. MEAD 1975 *Journal of Sound and Vibration* **40**, 1–18. Wave propagation and natural modes in periodic systems, I: mono-coupled systems.
3. P. W. ANDERSON 1958 *Physical Review* **109**, 1492–1505. Absence of diffusion in certain random lattices.
4. C. H. HODGES 1982 *Journal of Sound and Vibration* **82**, 411–424. Confinement of vibration by structural irregularity.
5. O. O. BENDIKSEN 1987 *American Institute of Aeronautics and Astronautics Journal* **25**, 1241–1248. Mode localization phenomena in large space structures.
6. C. H. HODGES and J. WOODHOUSE 1989 *Journal of Sound and Vibration* **130**, 237–251. Confinement of vibration by one-dimensional disorder, I: theory of ensemble averaging.
7. P. J. CORNWELL and O. O. BENDIKSEN 1989 *American Institute of Aeronautics and Astronautics Journal* **27**, 188–198. Forced vibrations in large space reflectors with localized modes.
8. S. D. LUST, P. P. FRIEDMANN and O. O. BENDIKSEN 1990 *American Institute of Aeronautics and Astronautics Journal* **28**, 225–235. Mode localization in multi-span beams.

9. C. PIERRE and E. H. DOWELL 1987 *Journal of Sound and Vibration* **114**, 549–564. Localization of vibrations by structural irregularity.
10. S. T. WEI and C. PIERRE 1988 *Journal of Vibration, Acoustics, Stress, and Reliability in Design* **110**, 439–449. Localization phenomena in mistuned assemblies with cyclic symmetry, part II: forced vibrations.
11. C. PIERRE, D. M. TANG and E. H. DOWELL 1987 *American Institute of Aeronautics and Astronautics Journal* **25**, 1249–1257. Localized vibrations of disordered multi-span beams: theory and experiment.
12. C. H. HODGES and J. WOODHOUSE 1983 *Journal of the Acoustical Society of America* **74**, 894–905. Vibration isolation from irregularity in a nearly periodic structure: Theory and measurements.
13. R. A. IBRAHIM 1987 *Applied Mechanics Reviews* **40**, 309–328. Structural dynamics with parameter uncertainties.
14. G. J. KISSEL 1988 *Ph.D. Dissertation, Massachusetts Institute of Technology*. Localization in disordered periodic structures.
15. P. D. CHA and C. PIERRE 1991 *Journal of Applied Mechanics* **58**, 1072–1081. Vibration localization by disorder in assemblies of monocoupled, multimode component systems.
16. C. PIERRE 1990 *Journal of Sound and Vibration* **139**, 111–132. Weak and strong vibration localization in disordered structures: a statistical investigation.
17. G. Q. CAI and Y. K. LIN 1991 *American Institute of Aeronautics and Astronautics Journal* **29**, 450–456. Localization of wave propagation in disordered periodic structures.
18. S. D. LUST, P. P. FRIEDMANN and O. O. BENDIKSEN 1991 *Proceedings of the 32nd AIAA/ASME/ASCE/AHS/ASC Structures, Structural Dynamics, and Materials Conference*, 2831–2842. Free and forced response of nearly periodic multi-span beams and multi-bay trusses.
19. F. Y. CHEN 1971 *Journal of Sound and Vibration* **14**, 57–79. On modeling and direct solution of certain free vibration systems.
20. C. H. HODGES and J. WOODHOUSE 1989 *Journal of Sound and Vibration* **130**, 253–268. Confinement of vibration by one-dimensional disorder, II: a numerical experiment on different ensemble averages.

APPENDIX: EXPONENTIAL DECAY CONSTANT

We define the ith bay of the oscillator chain as made of the ith oscillator and the coupling spring to its right. The bays are numbered such that bay $i+1$ is located to the right of bay i. Let us say that L_i and R_i are the complex amplitudes of the emergent left-travelling and incident right-travelling waves, respectively, at the ith bay. Let us also say that the transmission and reflection of waves at bay i is described by a transmission coefficient t_i, and a reflection coefficient r_i, which are independent of the direction of wave travel.

Using these conventions, we obtain the following relations

$$L_i = t_i L_{i+1} + r_i R_i, \qquad R_{i+1} = t_i R_i + r_i L_{i+1}, \tag{A1}$$

or, in matrix form,

$$\begin{bmatrix} L_i \\ R_{i+1} \end{bmatrix} = [S] \begin{bmatrix} L_{i+1} \\ R_i \end{bmatrix}, \qquad [S] = \begin{bmatrix} t_i & r_i \\ r_i & t_i \end{bmatrix}, \tag{A2}$$

where $[S]$ is called the scattering matrix.

With a little algebra, we can retrieve the following:

$$\begin{bmatrix} L_{i+1} \\ R_{i+1} \end{bmatrix} = [W_i] \begin{bmatrix} L_i \\ R_i \end{bmatrix}, \qquad [W_i] = \begin{bmatrix} 1/t_i & -r_i/t_i \\ r_i/t_i & t_i - r_i^2/t_i \end{bmatrix}. \tag{A3}$$

where $[W_i]$ is the wave transfer matrix for bay i. Note that $\det [W_i] \equiv 1$.

Now we consider N disordered oscillators in an otherwise infinite and ordered chain, with energy incident from the left of the first oscillator such that the amplitude of the right-travelling wave at oscillator 1 is R_1. The right-travelling wave which emerges from

the N-bay segment has amplitude R_{N+1}. Since there is no energy incident from the right of the system—that is, $L_{N+1}=0$—we find the following relationship

$$\begin{bmatrix} 0 \\ R_{N+1} \end{bmatrix} = [\mathscr{W}_N] \begin{bmatrix} L_1 \\ R_1 \end{bmatrix}, \tag{A4}$$

where $[\mathscr{W}_N]$ is the global wave transfer matrix for the N-bay segment. From equation (A3), it is clear that

$$[\mathscr{W}_N] = \prod_{i=N}^{1} [W_i]. \tag{A5}$$

Furthermore, the form of the global wave transfer matrix will be similar to that of the wave transfer matrix for site i: that is,

$$[\mathscr{W}_N] = \begin{bmatrix} 1/\tau_N & -\rho_N/\tau_N \\ \rho_N/\tau_N & \tau_N - \rho_N^2/\tau_N \end{bmatrix}, \tag{A6}$$

where τ_N and ρ_N are the transmission and reflection coefficients, respectively, of the N-bay segment.

By extracting and reducing the two algebraic equations of equation (A4), we can find that

$$R_{N+1} = \left([\mathscr{W}_N]_{(2,2)} - \frac{[\mathscr{W}_N]_{(2,1)}[\mathscr{W}_N]_{(1,2)}}{[\mathscr{W}_N]_{(1,1)}} \right) R_1. \tag{A7}$$

Therefore, the ratio of emergent to incident wave amplitudes is

$$R_{N+1}/R_1 = \det [\mathscr{W}_N]/[\mathscr{W}_N]_{(1,1)}. \tag{A8}$$

Since $[\mathscr{W}_N]$ is the product of matrices the determinants of which are equal to 1, we know that $\det[\mathscr{W}_N] \equiv 1$. Thus

$$R_{N+1}/R_1 = \frac{1}{[\mathscr{W}_N]_{(1,1)}}. \tag{A9}$$

Furthermore, let us assume that the spatial amplitude decay is asymptotically exponential. Therefore

$$R_{N+1}/R_1 \to e^{-\gamma N}, \qquad \text{as } N \to \infty, \tag{A10}$$

where γ is the exponential decay constant (the decay constant is simply the real part of the propagation constant, the imaginary part of which describes the phase change between bays). Using equations (A9) and (A10), we obtain

$$\gamma = \lim_{N\to\infty} \frac{1}{N} \ln |[\mathscr{W}_N]_{(1,1)}|, \tag{A11}$$

or, assuming ergodicity,

$$\gamma = \left\langle \frac{1}{N} \ln |[\mathscr{W}_N]_{(1,1)}| \right\rangle, \tag{A12}$$

where $\langle\ \rangle$ denotes an expected value.

Noting the form of $[\mathscr{W}_N]$ as shown in equation (A6), we can also express the decay constant in terms of the global transmission coefficient

$$\gamma = \lim_{N\to\infty} -(1/N) \ln |\tau_N|. \tag{A13}$$

Equations (A11)–(A13) are valid for all tuned and mistuned periodic systems coupled through one co-ordinate.

Now let us consider a system which has no disorder. In this case, there is no reflection of the energy-carrying waves, so $r_i = 0$, and the transmission coefficient is identical for all bays. Therefore, $t_i \equiv t_0$ for all i, and the wave transfer matrix is

$$[W_0] \equiv \begin{bmatrix} 1/t_0 & 0 \\ 0 & t_0 \end{bmatrix}. \tag{A14}$$

Using equation (A5), the global wave transfer matrix for a tuned N-bay segment is

$$[\mathscr{W}_N] = \begin{bmatrix} t_0^{-N} & 0 \\ 0 & t_0^{N} \end{bmatrix}. \tag{A15}$$

Finally, equations (A11) and (A15) lead to the relation

$$\gamma = -\ln |t_0|, \tag{A16}$$

which is valid for any tuned system.

Now we extend equation (A16) to the transfer matrix $[T_0]$, which relates the displacements of successive pairs of oscillators for a tuned system: that is,

$$\begin{bmatrix} u_{i+1} \\ u_i \end{bmatrix} = [T_0] \begin{bmatrix} u_i \\ u_{i-1} \end{bmatrix}. \tag{A17}$$

It is known that $[P]$, the matrix of eigenvectors of $[T_0]$, transforms the wave amplitudes to displacement amplitudes, such that

$$\begin{bmatrix} u_i \\ u_{i-1} \end{bmatrix} = [P] \begin{bmatrix} L_i \\ R_i \end{bmatrix}. \tag{A18}$$

Therefore, the displacement and wave transfer matrices are related by a similarity transformation

$$[T_0] = [P][W_0][P]^{-1}. \tag{A19}$$

Since $[W_0]$ and $[T_0]$ are similar matrices, they have the same eigenvalues. The eigenvalues of $[W_0]$ are obviously $1/t_0$ and t_0, which we now refer to as λ_1 and λ_2, respectively. We therefore rewrite equation (A16) as

$$\gamma = \ln |\lambda_1|. \tag{A20}$$

Since $|t_0| \leqslant 1$, we know that λ_1 is the eigenvalue of $[T_0]$ the modulus of which is greater than or equal to one.

Finally, we note that $\lambda_1 = 1/\lambda_2$. This reciprocal pair of eigenvalues is characteristic of a periodic system.